Thermal fluctuation conductivity and dimensionality in iron-based superconductors*

Rui Wang(王蕊)[1,2,†] and Ding-Ping Li(李定平)[1,2,‡]

[1] School of Physics, Peking University, Beijing 100871, China
[2] Collaborative Innovation Center of Quantum Matter, Beijing 100871, China

(Received 2 May 2016; revised manuscript received 6 June 2016; published online 19 July 2016)

The time-dependent Ginzburg–Landau Lawrence–Doniach model is used to investigate the superconducting fluctuation electrical conductivities. The theoretical result based on the self-consistent Gaussian approximation is used to fit the transport measurement data of iron-based superconductors F-doped LaOFeAs and $BaFe_{2-x}Ni_xAs_2$. We demonstrate that LaOFeAs shows layered behavior, while $BaFe_{2-x}Ni_xAs_2$ is more of a 3D feature. The conductivity in the region near T_c is well described by the theoretical formula.

Keywords: time-dependent Ginzburg–Landau Lawrence–Doniach model, iron-based superconductors, conductivity, dimensionality

PACS: 74.25.Ha, 74.40.–n, 74.70.Xa, 72.80.–r **DOI:** 10.1088/1674-1056/25/9/097401

1. Introduction

The iron-based superconductors have been investigated in depth both experimentally and theoretically.[1–7] Most of the iron pnictide superconductors have strong thermal fluctuations compared to most of the other superconductors (except cuprate superconductors) due to their large Ginzburg–Landau (GL) parameter κ, large critical temperature T_c, large anisotropy parameter γ, etc.[8] For different structures of iron pnictides, such as (1111), (111), (11), and (122) families, different dimensionality behaviors in the superconducting fluctuation region have been claimed.[9–16] However, the discussions for the dimensionality are still inconclusive. It was claimed that the superconducting fluctuation of LiFeAs followed the 2D behavior above T_c^{mf} in Ref. [11], but it was questioned in Ref. [17].

To describe the iron-based layered superconductors, we use the Lawrence–Doniach (LD) model, in which the original bulk expression is divided into two-dimensional (2D) superconducting layers with a Josephson coupling between them. The LD model describes well the experimental data of cuprate superconductors, for example, the data of the fluctuation conductivity and diamagnetisation.[18,19] Due to different temperatures and different magnetic fields, there exist 3D region, 2D region, and crossover region, which are shown in the vortex liquid state of the H–T phase diagram in Fig. 1. Region I (below T_c) is the 3D region. In region I, the coherence length along the c-axis is larger than the layer distance. Taking into account the 3D limit, where the layer distance can be taken to zero limit in the theoretical formula, the theoretical conductivity curves are almost the same as the original ones. Region III is the 2D region, where the coherence length is quite small compared to the layer distance. Region II is the crossover region between region I and region III, where the coherence length is on the same order with the layer distance. The larger anisotropy parameter, which leads to strong thermal fluctuation, may enhance the 2D and the crossover regions. Hence the strong anisotropy of the iron-based superconductors can enlarge both regions II and III in the H–T phase diagram compared to the less anisotropic superconductors.

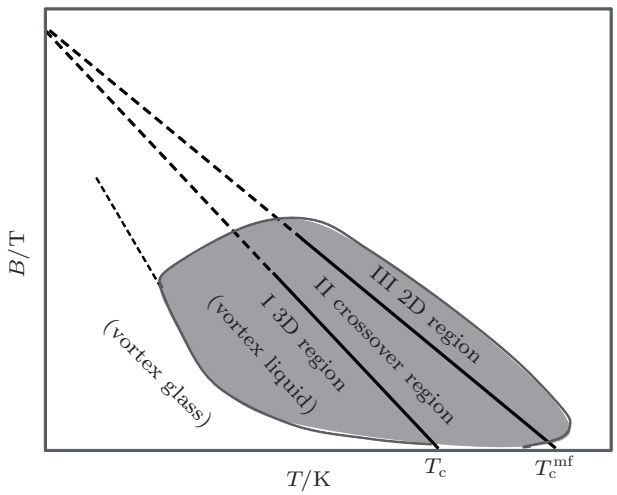


Fig. 1. The schematic H–T phase diagram. In the vortex liquid region, there are three regions, region I (the 3D region), region III (the 2D region), and region II (the crossover region). T_c is the transition temperature, T_c^{mf} is the mean-field transition temperature, and the upper critical magnetic field is $H_{c2} = T_c \frac{\partial H_{c2}}{\partial T}|_{T_c}$.

Both phenomenologic and microscopic multi-band theories have been developed to describe the experimental observation of the multi-band electronic structure in most of the

*Project supported by the National Natural Science Foundation of China (Grant No. 11274018).
†Corresponding author. E-mail: ruiwang95@126.com
‡Corresponding author. E-mail: lidp@pku.edu.cn
© 2016 Chinese Physical Society and IOP Publishing Ltd

iron pnictides families, such as (1111), (11), (111), and (122) families.[20–22] However, the single-band model can be used approximately near T_c.[23] We use the single-band LD model in this paper to study the fluctuation conductivity of vortex liquid near T_c. The often used method describing the fluctuation properties of superconductivity is Gaussian fluctuation theory (GFT),[13,15,24,25] in which the quartic term of the GL free energy is omitted. The GFT method can only describe region III in Fig. 1. The self-consistent approximation[18,19] was developed and was used to explain the various experimental data, like conductivity and diamagnetisation of vortex liquid. In the self-consistent Gaussian theory (SCGT), the quartic term is taken into account in the Hartree–Fock approximation. The SCGT can describe all three regions in Fig. 1.

This paper is organized as follows. In Section 2, the calculation of the superconducting fluctuation conductivity based on the time-dependent Ginzburg–Landau (TDGL) function with the linear response approach under the self-consistent approximation is briefly introduced. In Section 3, we present the theoretical fitting of the experimental conductivity data and the discussion. We summarize and conclude in Section 4.

2. Fluctuation conductivity based on the TDGL model

The mean-field GL free energy of the LD model is

$$F_{\rm GL} = d'\sum_n \int {\rm d}^2 r\left(\frac{\hbar^2}{2m^*}|\boldsymbol{D}\Psi_n|^2+\frac{\hbar^2}{2m_c d'^2}|\Psi_n-\Psi_{n+1}|^2 + a|\Psi_n|^2+\frac{b'}{2}|\Psi_n|^4\right), \quad (1)$$

where d' is the distance between layers labeled by n, m^* is the effective Cooper pair mass in the ab plane, and m_c is the effective Cooper pair mass along the c axis. The anisotropy parameter γ is denoted as the ratio of the effective masses along the two different orientations, $\gamma=\sqrt{m_c/m^*}$. $a=\alpha(T-T_{\rm c}^{\rm mf})=\alpha T_{\rm c}^{\rm mf}(t^{\rm mf}-1)$, where $t^{\rm mf}=T/T_{\rm c}^{\rm mf}$, in which $T_{\rm c}^{\rm mf}$ is the mean-field critical temperature. The covariant derivative is defined by $\boldsymbol{D}=\nabla+{\rm i}2\pi/\phi_0\boldsymbol{A}$. The superfluxon is $\phi_0=hc/2e$ with electric charge $e=|e|$. The ratio of the coherence length $\xi^2=\hbar^2/(2m^*\alpha T_{\rm c})$ and the penetration depth $\lambda^2=c^2m^*b'/(16\pi e^2\alpha T_{\rm c})$ describes the Ginzburg Landau parameter $\kappa=\lambda/\xi$, which is very large for iron pnictides. We will consider a constant external magnetic field. Due to large κ, the diamagnetization is $B-H\propto H/\kappa^2\to B\simeq H$. Hence we can choose $\boldsymbol{A}=(-By,0)$, where $B=H$, and assume that the magnetic field is orientated along the crystallographic c axis. The supercurrent in the original unit is given by the GL theory

$$j'_{n,s}=\frac{{\rm i}e\hbar}{m^*}\left(\Psi_n^*\boldsymbol{D}\Psi_n-\Psi_n\boldsymbol{D}\Psi_n^*\right). \quad (2)$$

2.1. TDGL model

To describe the transport properties of the layered iron-based superconductors, the TDGL equation will be used, i.e.,

$$\frac{\hbar^2\gamma'}{2m^*}D_\tau\Psi_n=-\frac{1}{d'}\frac{\delta F_{\rm GL}}{\delta\Psi_n^*}+\zeta_n, \quad (3)$$

where $D_\tau=(\partial_\tau-{\rm i}(2e/\hbar)\Phi)$ is the covariant time derivative, in which the scalar electric potential is $\Phi=-E'y$. The electric field is therefore assumed to orientate along the y axis. The inverse diffusion constant $\gamma'/2$ is assumed to be real, as we can neglect the tiny imaginary part of γ', which has to be included when the Hall conductivity and Seebeck effect are considered.[19] ζ_n is the thermal noise,[26] which satisfies

$$\left\langle\zeta_n^*(\boldsymbol{r},\tau)\,\zeta_m\left(\boldsymbol{r}',\tau'\right)\right\rangle_{\rm th}=\frac{\hbar^2\gamma'}{m^*d'}T\delta\left(\boldsymbol{r}-r'\right)\delta\left(\tau-\tau'\right)\delta_{nm}, \quad (4)$$

where $\langle\cdots\rangle_{\rm th}$ is the thermal average. We substitute Eq. (1) into Eq. (3) and obtain

$$\begin{aligned}&\frac{1}{d'}\frac{\delta F_{\rm GL}}{\delta\psi_n^*(\boldsymbol{r},\tau)}\\ &=-\frac{\hbar^2}{2m^*}\left(\nabla-{\rm i}\frac{2\pi}{\phi_0}\boldsymbol{A}(\boldsymbol{r},\tau)\right)^2\psi_n(\boldsymbol{r},\tau)\\ &\quad+\frac{\hbar^2}{2m_cd'^2}\left[2\psi_n(\boldsymbol{r},\tau)-\psi_{n+1}(\boldsymbol{r},\tau)-\psi_{n-1}(\boldsymbol{r},\tau)\right]\\ &\quad+a\psi_n(\boldsymbol{r},\tau)+b'|\psi_n(\boldsymbol{r},\tau)|^2\psi_n(\boldsymbol{r},\tau), \end{aligned} \quad (5)$$

where $|\psi_n(\boldsymbol{r},\tau)|^2\psi_n(\boldsymbol{r},\tau)$ will be substituted by $2\langle|\psi_n(\boldsymbol{r},\tau)|^2\rangle\psi_n(\boldsymbol{r},\tau)$ using the Hartree–Fock approximation, and $\langle\cdots\rangle$ means that we take thermal and space-time average if not specified.

The physical units will be used to make the model and equations dimensionless. The coherence length ξ will be used as the unit of length and the upper critical field $H_{\rm c2}\equiv\hbar c/2e\xi^2$ as the magnetic field unit. The dimensionless order parameter is $\psi_n=\sqrt{b'/2\alpha T_{\rm c}^{\rm mf}}\Psi_n$. The TDGL equation will take the dimensionless form

$$\begin{aligned}&D_\tau\psi_n(\boldsymbol{r},\tau)\\ &=\left(\frac{1}{2}\boldsymbol{D}^2+\frac{b}{2}\right)\psi_n(\boldsymbol{r},\tau)-\frac{1}{2d^2}[2\psi_n(\boldsymbol{r},\tau)\\ &\quad-\psi_{n+1}(\boldsymbol{r},\tau)-\psi_{n-1}(\boldsymbol{r},\tau)]-\varepsilon\psi_n(\boldsymbol{r},\tau)+\zeta_n, \end{aligned} \quad (6)$$

where $\varepsilon=-a_{\rm h}+2\langle|\psi_n(\boldsymbol{r},\tau)|^2\rangle$ and $a_{\rm h}=\left(1-t^{\rm mf}-b\right)/2$. The covariant derivative is $\boldsymbol{D}=(\partial/\partial x-{\rm i}by)\boldsymbol{i}+\partial/\partial y\boldsymbol{j}$, in which the dimensionless magnetic field is $b=B/H_{\rm c2}$. The dimensionless covariant time derivative is $D_\tau=(\partial_\tau+{\rm i}Ey)$, in which the electric field $E=E'/E_{\rm GL}$ is scaled with the unit $E_{\rm GL}=H_{\rm c2}\xi/c\tau_{\rm GL}$. $\tau_{\rm GL}$ is a typical "relaxation" time in the superconducting phase, $\tau_{\rm GL}=\gamma'\xi^2/2$. The layer distance d ($d=d'/\xi_{\rm c}$) is rescaled with the coherence length in the c axis, $\xi_{\rm c}=\xi/\gamma$ ($\gamma=\sqrt{m_c/m^*}$). The dimensionless Gaussian white noise takes the form

$$\left\langle\zeta_n^*(\boldsymbol{r},\tau)\,\zeta_m\left(\boldsymbol{r}',\tau'\right)\right\rangle_{\rm th}$$

$$= \frac{2\omega^{\rm mf} t^{\rm mf}}{d}\delta\left(\boldsymbol{r}-\boldsymbol{r}'\right)\delta\left(\tau-\tau'\right)\delta_{nm}, \tag{7}$$

where $\omega^{\rm mf}$ is the fluctuation strength, $\omega^{\rm mf} = \sqrt{2G_{\rm i}^{\rm mf}}\pi$, and $G_{\rm i}^{\rm mf}$ is the customary Ginzburg number, $G_{\rm i}^{\rm mf} = 4(e/c\hbar)^3\kappa^4 T_{\rm c}^{\rm mf2}\gamma^2/H_{\rm c2}$.

The $\langle|\psi_n(\boldsymbol{r},\tau)|^2\rangle$ can be calculated by solving Eq. (6), and ε can be obtained self-consistently by the gap equation[18,19]

$$\varepsilon = -a_{\rm h} + 2\left\langle|\psi_n(\boldsymbol{r},\tau)|^2\right\rangle. \tag{8}$$

The dimensionless supercurrent density takes the form

$$\boldsymbol{J}_{\rm s} = \frac{\rm i}{2}\langle\psi_n^*\boldsymbol{D}\psi_n\rangle + {\rm c.c.} \tag{9}$$

with the unit of the current density, $j_{\rm GL} = H_{\rm c2}c/2\pi\kappa^2\xi$. The conductivity will be given in units of $\sigma_{\rm GL} = j_{\rm GL}/E_{\rm GL} = c^2\gamma'/4\pi\kappa^2$.

2.2. Calculation of the conductivity

The linear response theory is used to calculate the superconducting fluctuation conductivity $\sigma_{\rm s}$. The total electrical conductivity is $\sigma = \sigma_{\rm n} + \sigma_{\rm s}$, where $\sigma_{\rm n}$ is the normal conductivity.

To solve the linearized TDGL Eq. (6), we use the Fourier transform

$$\begin{aligned}\psi_n(\boldsymbol{r},\tau) &= \int_0^{2\pi/d}\frac{{\rm d}k_z}{2\pi}{\rm e}^{-{\rm i}nk_z d}\psi_{kz}(\boldsymbol{r},\tau),\\ \zeta_n &= \int_0^{2\pi/d}\frac{{\rm d}k_z}{2\pi}{\rm e}^{-{\rm i}nk_z d}\zeta_{kz}(\boldsymbol{r},\tau).\end{aligned} \tag{10}$$

The TDGL equation becomes

$$\begin{aligned}&\left\{D_\tau - \left(\frac{1}{2}\boldsymbol{D}^2 + \frac{b}{2}\right) + \frac{1}{d^2}(1-\cos k_z d) + \varepsilon\right\}\psi_{kz}(\boldsymbol{r},\tau)\\ &= \zeta_{kz}(\boldsymbol{r},\tau),\end{aligned} \tag{11}$$

where

$$\begin{aligned}&\left\langle\zeta_{kz}^*(\boldsymbol{r},\tau)\zeta_{k'z}\left(\boldsymbol{r}',\tau'\right)\right\rangle_{\rm th}\\ &= 4\pi\omega^{\rm mf}t^{\rm mf}\delta\left(\boldsymbol{r}-\boldsymbol{r}'\right)\delta\left(\tau-\tau'\right)\delta\left(k_z-k_z'\right).\end{aligned} \tag{12}$$

Then the TDGL equation is rewritten as

$$\left(\widehat{L}^{-1} + {\rm i}Ey\right)\psi_{kz}(r,\tau) = \zeta_{k_z}(r,\tau), \tag{13}$$

where $\psi_{kz}(r,\tau)$ can be expended to the linear order of the electric field, i.e.,

$$\psi_{kz}(r,\tau) = \psi_{0k_z}(r,\tau) + \psi_{1k_z}(r,\tau), \tag{14}$$

and

$$\widehat{L}^{-1} = \partial_\tau - \frac{1}{2}D^2 - \frac{b}{2} + \varepsilon + j(k_z), \tag{15}$$

in which $j(k_z)$ is denoted as $j(k_z) = \frac{1}{d^2}[1-\cos(k_z d)]$. The zero order and the first order equations are solved as follows:

$$\psi_{0k_z}(r,\tau) = \widehat{L}\zeta_{k_z}(r,\tau), \tag{16}$$

$$\psi_{1k_z}(r,\tau) = -{\rm i}E\widehat{L}y\psi_{0k_z}(r,\tau). \tag{17}$$

The supercurrent in the y direction is obtained in the Fourier form

$$\begin{aligned}J_y^{\rm e} = \frac{\rm i}{2}&\int_0^{2\pi/d}\frac{{\rm d}k_z}{2\pi}\int_0^{2\pi/d}\frac{{\rm d}k_z'}{2\pi}{\rm e}^{{\rm i}n\left(k_z-k_z'\right)d}\\ &\times\left\langle\psi_{k_z}^*(r,\tau)\frac{\partial}{\partial y}\psi_{k_z'}(r,\tau)\right\rangle + {\rm c.c.}\end{aligned} \tag{18}$$

We substitute Eqs. (16) and (17) into the supercurrent Eq. (18), and only keep the terms with zero order and first order of E. Then the supercurrent takes the form

$$\begin{aligned}J_y^{\rm e} &= {\rm Re}\left[{\rm i}\int_0^{2\pi/d}\frac{{\rm d}k_z}{2\pi}\frac{{\rm d}k_z'}{2\pi}{\rm e}^{{\rm i}n\left(k_z-k_z'\right)d}\right.\\ &\quad\left.\times\left\langle\psi_{0k_z}^*(r,\tau)\frac{\partial}{\partial y}\psi_{0k_z'}(r,\tau)\right\rangle\right]\\ &\quad -2E\,{\rm Re}\left[\int_0^{2\pi/d}\frac{{\rm d}k_z}{2\pi}\frac{{\rm d}k_z'}{2\pi}{\rm e}^{{\rm i}n\left(k_z-k_z'\right)d}\right.\\ &\quad\left.\times\left\langle\psi_{0k_z}^*(r,\tau)y\widehat{L}^\dagger\frac{\partial}{\partial y}\psi_{0k_z'}(r,\tau)\right\rangle\right]\\ &= j_{y0}^{\rm e} + j_{y1}^{\rm e}.\end{aligned} \tag{19}$$

The first term in the above equation is the supercurrent of the equilibrium state, which equals to zero, and we only need calculate the second term. In order to calculate $j_{y1}^{\rm e}$, the following eigenfunction of $\widehat{L}^{-1}$ will be used:[24]

$$\begin{aligned}\widehat{L}^{-1}\varphi_l(r,\tau) &= E_l\varphi_l(r,\tau),\\ \varphi_{l,k,\Omega}(r,\tau) &= \frac{1}{\sqrt{t^* L_x}}\chi_l(y)\,{\rm e}^{-{\rm i}(kx-\Omega\tau)},\end{aligned} \tag{20}$$

where L_x is the sample length along the x direction, t^* is the time period, k, Ω, and l are discrete quantum numbers, and

$$\begin{aligned}\chi_l(y) &= \left(\frac{b}{\pi}\right)^{1/4}\left(\frac{1}{2^l l!}\right)^{1/2}\\ &\quad\times\exp\left[-\frac{1}{2}\left(\sqrt{b}y + \frac{k}{\sqrt{b}}\right)^2\right]H_l\left(\sqrt{b}y + \frac{k}{\sqrt{b}}\right),\\ E_l &= lb + \varepsilon + j(k_z) + {\rm i}\Omega.\end{aligned} \tag{21}$$

Equation (18) can be solved by the insertion of complete set $\sum_l|\varphi_l\rangle\langle\varphi_l|$, in which all the Landau levels are added. Here we take $l = (l,k,\Omega)$ for simplicity. The supercurrent density becomes[24]

$$\begin{aligned}j_{y1}^{\rm e} &= -2E\,{\rm Re}\left\langle\int_0^{2\pi/d}\frac{{\rm d}k_z}{2\pi}\frac{{\rm d}k_z'}{2\pi}{\rm e}^{{\rm i}n\left(k_z-k_z'\right)d}\right.\\ &\quad\times\sum_{l_1,\ldots,l_6}\frac{1}{t^* L_x L_y}\langle\zeta_{k_z}^*|\varphi_{l_6}\rangle\langle\varphi_{l_6}|\widehat{L}^\dagger|\varphi_{l_5}\rangle\langle\varphi_{l_5}|y|\varphi_{l_4}\rangle\\ &\quad\left.\times\langle\varphi_{l_4}|\widehat{L}^\dagger|\varphi_{l_3}\rangle\langle\varphi_{l_3}\left|\frac{\partial}{\partial y}\right|\varphi_{l_2}\rangle\langle\varphi_{l_2}|\widehat{L}|\varphi_{l_1}\rangle\langle\varphi_{l_1}|\zeta_{k_z'}\rangle\right\rangle_{\rm th},\end{aligned} \tag{22}$$

where the factor $\frac{1}{t^* L_x L_y}$ is used to take space–time average of the supercurrent, and the Dirac bra–ket $\langle F_1 \left| \widehat{O} \right| F_2 \rangle$ of the quantum mechanics matrix element is used for facilitating the calculation. The matrix elements in Eq. (22) need to be solved first. Since φ_l is the eigenfunction of operator $\widehat{L}^{-1}$, the matrix elements $\langle \varphi_{l_6} \widehat{L}^{\dagger} \varphi_{l_5} \rangle$, $\langle \varphi_{l_2} \widehat{L} \varphi_{l_1} \rangle$, and $\langle \varphi_{l_3} \left| \frac{\partial}{\partial y} \right| \varphi_{l_2} \rangle$ can be calculated easily with Eq. (20) and quantum mechanics of Landau levels.

Discrete summations can be transferred to integration $\sum_{\Omega,k} \to \int \frac{t^* \mathrm{d}\Omega}{2\pi} \int_0^{bL_y} \frac{L_x \mathrm{d}k}{2\pi}$. The supercurrent therefore takes the form

$$\begin{aligned} j_{y1}^{\mathrm{e}} &= -2E \int_0^{2\pi/d} \frac{\mathrm{d}k_z}{(2\pi)^2} 4\pi \omega^{\mathrm{mf}} t^{\mathrm{mf}} \frac{bL_x L_y}{2\pi} \frac{1}{L_x L_y} \\ &\times \frac{1}{b} \sum_{l,l'} \left[\left(\frac{l+1}{2} \right)^{1/2} \delta_{l+1,l'} + \left(\frac{l}{2} \right)^{1/2} \delta_{l-1,l'} \right] \\ &\times \left[- \left(\frac{l+1}{2} \right)^{1/2} \delta_{l+1,l'} + \left(\frac{l}{2} \right)^{1/2} \delta_{l-1,l'} \right] \\ &\int \frac{\mathrm{d}\Omega}{2\pi} \frac{1}{E_{l'}^*} \left| \frac{1}{E_l} \right|^2, \end{aligned} \tag{23}$$

and the integration of Ω is

$$\begin{aligned} &\int \mathrm{d}\Omega \frac{1}{E_{l'}^*} \left| \frac{1}{E_l} \right|^2 \\ &= \frac{\pi}{\left[(l'+l)b + 2\varepsilon + 2j(k_z) \right]} \frac{1}{\left[lb + \varepsilon + j(k_z) \right]}. \end{aligned} \tag{24}$$

The supercurrent becomes

$$\begin{aligned} j_{y1}^{\mathrm{e}} &= \frac{E\omega^{\mathrm{mf}} t^{\mathrm{mf}}}{4\pi^2 b} \int_0^{2\pi/d} \mathrm{d}k_z \left\{ \sum_{l=0}^{N_{\mathrm{f}}} \left[\frac{(2l+1)b}{\left[lb + \varepsilon + j(k_z) \right]} \right. \right. \\ &\left. - \frac{2(l+1)b}{(l+1/2)b + \varepsilon + j(k_z)} \right] \\ &\left. + \frac{(N_{\mathrm{f}}+1)b}{(N_{\mathrm{f}}+1/2)b + \varepsilon + j(k_z)} \right\}, \end{aligned} \tag{25}$$

in which cutoff (N_{f}) of the Landau levels is imposed. The final result is $j_y = \sigma_{\mathrm{s}} E$, and

$$\begin{aligned} \sigma_{\mathrm{s}} &= \frac{\omega^{\mathrm{mf}} t^{\mathrm{mf}}}{2\pi^2 b} \int_0^{2\pi/d} \mathrm{d}k_z \frac{\left[\varepsilon + j(k_z) \right] - b/2}{b} \\ &\times \left\{ \psi\left(\left[\varepsilon + j(k_z) \right]/b \right) - \psi\left(\left[\Lambda + \varepsilon + j(k_z) \right]/b \right) \right. \\ &- \psi\left(\left[\varepsilon + j(k_z) \right]/b + 1/2 \right) \\ &+ \psi\left(\left[\Lambda + \varepsilon + j(k_z) \right]/b + 1/2 \right) \\ &\left. + \frac{\Lambda/2}{\left[\Lambda + \varepsilon + j(k_z) - b/2 \right]} \frac{b}{\left[\varepsilon + j(k_z) \right] - b/2} \right\}. \end{aligned} \tag{26}$$

Here the ultra-violet cutoff is defined as $\Lambda = (N_{\mathrm{f}}+1)b$ and the cutoff Λ is the depairing energy of Cooper pairs. Compared to the inter- and intra-Landau-level excitation energy scales in dimensionless units, i.e., b and ε, Λ is sufficiently large near T_{c}, so the expression of the supercurrent can be weakly cutoff independent. σ_{s} is consistent with the solution of the Green function method, when cutoff Λ approaches infinity.[19]

2.3. Renormalization

The self-consistent equation ε is solved by substituting Eqs. (14), (16), and (17) into Eq. (8)

$$\begin{aligned} \varepsilon &= -a_{\mathrm{h}} + 2 \int_0^{2\pi/d} \frac{\mathrm{d}k_z'}{2\pi} \frac{\mathrm{d}k_z}{2\pi} \mathrm{e}^{\mathrm{i}n\left(k_z' - k_z\right)} \\ &\times \left\langle \zeta_{k_z'}^*(r,\tau) \widehat{L}^{\dagger} \widehat{L} \zeta_{k_z}(r,\tau) \right\rangle. \end{aligned} \tag{27}$$

The $\langle \cdots \rangle$ can be calculated following the similar steps in the last subsection, and the result is

$$\begin{aligned} \varepsilon &= -a_{\mathrm{h}} + 2\omega^{\mathrm{mf}} t^{\mathrm{mf}} \int_0^{2\pi/d} \frac{\mathrm{d}k_z}{(2\pi)^2} \left[\psi\left(\frac{\varepsilon + j(k_z) + \Lambda}{b} \right) \right. \\ &\left. - \psi\left(\frac{\varepsilon + j(k_z)}{b} \right) \right], \end{aligned} \tag{28}$$

which was derived in Ref. [18] where the thermodynamic properties were studied based on the GL model.

The real critical temperature T_{c} can be defined at $\varepsilon = 0$ when the magnetic field is zero. By taking the limit $b \to 0$, the above equation gives

$$T_{\mathrm{c}}^{\mathrm{mf}} = \frac{T_{\mathrm{c}}}{1 - 4\omega U_0}, \tag{29}$$

where $\omega = \sqrt{2G\mathrm{i}}\pi$, $G\mathrm{i} = 4(e/c\hbar)^3 \kappa^4 T_{\mathrm{c}}^2 \gamma^2 / H_{\mathrm{c2}}$, and

$$U_0 = \frac{1}{2\pi d} \left[\ln\left(\Lambda d^2 + 1 + d\sqrt{\Lambda\left(\Lambda d^2 + 2\right)} \right) \right].$$

Substituting Eq. (29) into Eq. (28), we obtain the gap equation

$$\varepsilon = -a_{\mathrm{h}}^{\mathrm{r}} + 2\omega t \left(U_\varepsilon - U_0 \right), \tag{30}$$

where

$$\begin{aligned} U_\varepsilon &= \int_0^{2\pi/d} \frac{\mathrm{d}k_z}{(2\pi)^2} \left[\psi\left(\left[\varepsilon + j(k_z) \right]/b + \Lambda/b \right) \right. \\ &\left. - \psi\left(\left[\varepsilon + j(k_z) \right]/b \right) \right], \end{aligned} \tag{31}$$

and $a_{\mathrm{h}}^{\mathrm{r}} = (1 - t - b)/2$ with $t = T/T_{\mathrm{c}}$. It is easy to prove $\omega t = \omega^{\mathrm{mf}} t^{\mathrm{mf}}$. The ε in Eq. (30) can be solved self-consistently, and it shall be positive definite due to the positive requirement of the variational free energy.[18]

2.4. 3D limit and renormalization

By taking the 3D limit of Eq. (26),

$$\begin{aligned} &\sigma_{\mathrm{s}(d\to 0)} \\ &= \frac{\omega t}{2\pi^2 b} \int_{-\infty}^{\infty} \mathrm{d}k_z \frac{\left[\varepsilon + k_z^2/2 \right] - b/2}{b} \\ &\times \left\{ \psi\left(\left[\varepsilon + \frac{k_z^2}{2} \right]/b \right) - \psi\left(\left[\Lambda + \varepsilon + \frac{k_z^2}{2} \right]/b \right) \right. \\ &- \psi\left(\left[\varepsilon + \frac{k_z^2}{2} \right]/b + \frac{1}{2} \right) + \psi\left(\left[\Lambda + \varepsilon + \frac{k_z^2}{2} \right]/b + \frac{1}{2} \right) \\ &\left. + \frac{\Lambda/2}{\left[\Lambda + \varepsilon + k_z^2/2 - b/2 \right]} \frac{b}{\left[\varepsilon + k_z^2/2 \right] - b/2} \right\}. \end{aligned} \tag{32}$$

The self-consistent equation in the 3D limit is therefore

$$\varepsilon_{d\to 0} = -a_{\rm h}^{\rm r} + 2\omega t\,(U_\varepsilon(d\to 0) - U_0(d\to 0))\,, \qquad (33)$$

where $U_0(d\to 0)$ and $U_\varepsilon(d\to 0)$ are

$$\begin{aligned} U_0(d\to 0) &= \frac{\sqrt{2\Lambda}}{2\pi}, \\ U_\varepsilon(d\to 0) &= \int_{-\infty}^{\infty} \frac{{\rm d}k}{(2\pi)^2}\left[\psi\left(\frac{\varepsilon + k^2/2 + \Lambda}{b}\right)\right. \\ &\quad \left. - \psi\left(\frac{\varepsilon + k^2/2}{b}\right)\right] \end{aligned} \qquad (34)$$

by taking the limit of $d\to 0$.

3. Experimental data fitting

The superconducting fluctuation conductivities of both the F-doped LaOFeAs compound ($T_{\rm c} = 19.8$ K, 1111 family)[27] and the single crystal $BaFe_{2-x}Ni_xAs_2$ ($T_{\rm c} = 20$ K, 122 family)[25] are fitted in Fig. 2. The fitting parameters are listed in Table 1.

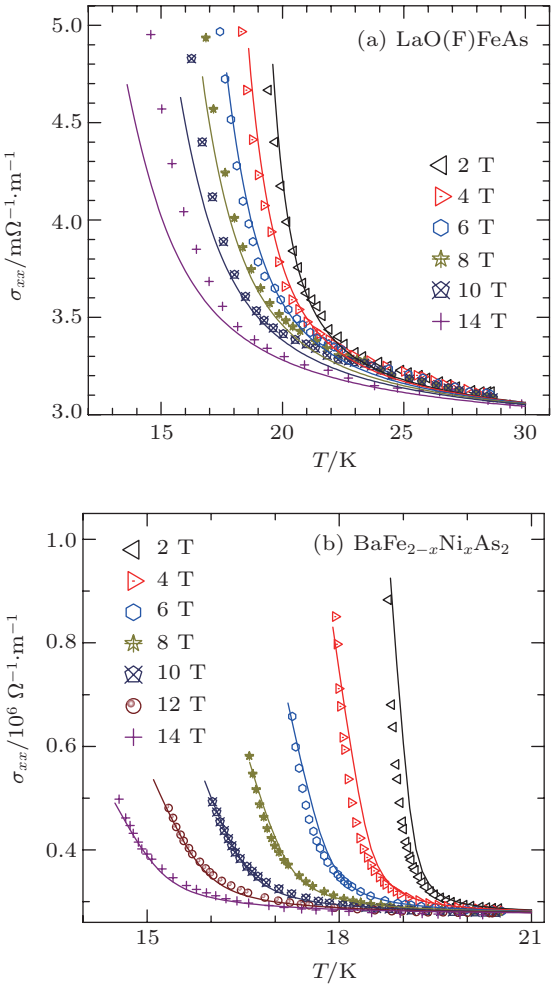


Fig. 2. (color online) The superconducting fluctuation electrical conductivities of (a) the F-doped compound LaOFeAs and (b) the single crystal $BaFe_{2-x}Ni_xAs_2$. The lines are given by the theoretical fitting formula Eq. (26) of conductivity under different magnetic fields. The points are taken from the experimental data.

Table 1. The fitting parameters for LaOFeAs and $BaFe_{2-x}Ni_xAs_2$.

Material	$G_{\rm i}$	γ	$H_{\rm c2}$	$T_{\rm c}$	$\xi_{\rm c}$	d'
LaO(F)FeAs	0.0015	7.64	50 T	20 K	3.35 Å	8.717 Å
$BaFe_{2-x}Ni_xAs_2$	0.00002	2.076	61.65 T	19.8 K	11.1 Å	6.36 Å

3.1. LaOFeAs

The layer distance d' of LaOFeAs used in the calculation is $d' = 8.717$ Å. The expression of relaxation time γ' in BCS, $\gamma'_{\rm BCS} = \frac{\pi\hbar}{8k_{\rm B}T_{\rm c}\xi}$, is derived for BCS superconductors. For high-$T_{\rm c}$ superconductors, we denote $\gamma' = \gamma'_{\rm n}\gamma'_{\rm BCS}$, where constant $\gamma'_{\rm n}$ may not equal to one and will be determined by data fitting. The conductivity $\sigma = \sigma_{\rm s} + \sigma_{\rm n}$, reciprocal to the original experimental resistivity data, is fitted using Eq. (26). $\sigma_{\rm n} = 2.86$ ${\rm m}\Omega^{-1}\cdot{\rm cm}^{-1}$ according to the experimental data.[27] The cut-off Λ is set to be 0.3, which is approximately in the same order as used in Ref. [25]. The absolute value of Λ is not sensitive to the calculation in regions I and II (see Fig.1) due to $\varepsilon, b \ll \Lambda$.

The fitting parameters are chosen as $\gamma'_{\rm n} = 0.7$, $H_{\rm c2} = T_{\rm c}\frac{\partial H_{\rm c2}(T)}{\partial T}|_{T_{\rm c}} = 50$ T, the anisotropy parameter $\gamma = 7.64$, and the Ginzburg–Landau parameter $\kappa = 73.36$, which are basically consistent with Refs. [28] and [29]. Based on the fitting parameters, Ginzburg number $G_{\rm i} = 4(e/c\hbar)^3\kappa^4 T_{\rm c}^2\gamma^2/H_{\rm c2} = 0.0015$, and the fluctuation strength parameter $\omega = \sqrt{2G_{\rm i}}\pi = 0.17$ $G_{\rm i}$ is in the same order of magnitude with that of cuprate YBaCuO,[19] which suggests that they may have the same order of fluctuation strength. The dimensionless layer distance $d = 2.6$ for LaOFeAs demonstrates a relatively layered behavior.[9] Furthermore, the mean-field critical temperature $T_{\rm c}^{\rm mf} = 21.5$ K, calculated with Eq. (29), is close to the onset critical temperature measured in experiment $T_{\rm c}^{\rm onset}$. $T_{\rm c}^{\rm mf} - T_{\rm c} = 1.5$ K, which is relatively large in iron pnictide superconductors. Therefore, the crossover region and the 2D region, i.e., regions II and III in Fig. 1, are larger than those of the other iron pnictide families, like $BaFe_{2-x}Ni_xAs_2$, which will be discussed later. From Fig. 2(a), we can see that this material has a large temperature transition region, which is corresponding to the 2D–3D crossover region in Fig. 1. So LaOFeAs shows a layered characteristic in a relatively wider range of temperatures and magnetic fields compared to $BaFe_{2-x}Ni_xAs_2$.

3.2. $BaFe_{2-x}Ni_xAs_2$

For $BaFe_{2-x}Ni_xAs_2$, the layer distance is $d' = 6.36$ Å. The normal conductivity $\sigma_{\rm n} = 0.027\times 10^7\ \Omega^{-1}\cdot{\rm m}^{-1}$ is taken to be constant by ignoring the tiny dependence of $\sigma_{\rm n}$ on the magnetic field as shown in Ref. [25].

The fitting parameters are $\gamma'_{\rm n} = 0.56$, $\gamma = 2.076$, $\kappa = 52.9$, and $H_{\rm c2} = 61.65$ T, which are consistent with Refs. [25] and [30]. Thus, the Ginzburg number $G_{\rm i} = 0.00002$ is rather small compared to that of LaOFeAs, indicating a relatively

weak fluctuation effect for $BaFe_{2-x}Ni_xAs_2$. The dimensionless layer distance $d = 0.57$ indicates that $BaFe_{2-x}Ni_xAs_2$ has a 3D characteristic. Furthermore, when we take 3D limit $d \to 0$ in the numerical calculation, it is hard to find any difference from the previous result, suggesting a 3D behavior for $BaFe_{2-x}Ni_xAs_2$. Besides, the mean-field critical temperature T_c^{mf} calculated from Eq. (29) is $T_c^{mf} = 20$ K. $T_c^{mf} - T_c = 0.2$ K, which is much smaller than that of LaOFeAs. Therefore, the crossover region and the 2D region are much smaller than those of LaOFeAs, and it shows that $BaFe_{2-x}Ni_xAs_2$ is dominated by the 3D behavior (region I in Fig. 1).

3.3. Discussion

In order to clarify the dimensionality of the ion-based superconductors, we need to compare the coherence length and the layer distance in the c axis $\xi_c(T,B)$. $\xi_c(T,B)$ is dependent on the magnetic fields and temperatures, which is not easy to obtain from the theoretical equations. Dimensionless coherence length in the c axis $\xi_c(T,B)/\xi_c$ is approximately in the same order of magnitude as $1/\sqrt{\varepsilon}$, in which ε is calculated numerically from Eq. (30) with the parameters listed in Table 1. Comparing ε and $1/d^2$, we find that the iron pnictides can be classified by their dimensionality, as shown in Fig. 1 for three regions, i.e., region I is of the 3D feature, region III is of the 2D feature, and region II is the crossover region.

The information about the coupling between the nearest layers can be described by the Josephson coupling parameter, $\Gamma = \frac{\langle|\psi_n - \psi_{n-1}|^2\rangle}{\langle|\psi_n|^2\rangle}$. Γ is of the order of $e^{-\alpha d\sqrt{\varepsilon}}$, where α is of the order of 1.[31] When $\varepsilon d^2 \gg 1$, the coupling between the layers is weak, so the sample is of the 2D feature. If $\varepsilon d^2 \ll 1$, the coupling between the layers is strong, therefore the sample is of the 3D feature. When εd^2 is of the order of 1, the sample shows a layered behavior.

In zero magnetic field, if we take the 2D limit ($\varepsilon d^2 \gg 1$) and the 3D limit ($\varepsilon d^2 \ll 1$) of Eq. (26) respectively, we can obtain the same expression with the Aslamazov–Larkin theory of the excess conductivity, $\sigma_{s2D} \propto \varepsilon^{-1}$ and $\sigma_{s3D} \propto \varepsilon^{-1/2}$.[24,32] The experimental study of dimensionality of conductivity in cuprate superconductor can be found in Refs. [33]–[35].

Figures (a)and (b) show the contour lines of εd^2 as a function of temperatures and magnetic fields for $BaFe_{2-x}Ni_xAs_2$ and LaOFeAs. For LaOFeAs, $\varepsilon d^2 \sim 1$, it indicates that this material has a layered feature. For $BaFe_{2-x}Ni_xAs_2$, $\varepsilon d^2 \ll 1$, we contribute this material to the 3D bulk category.

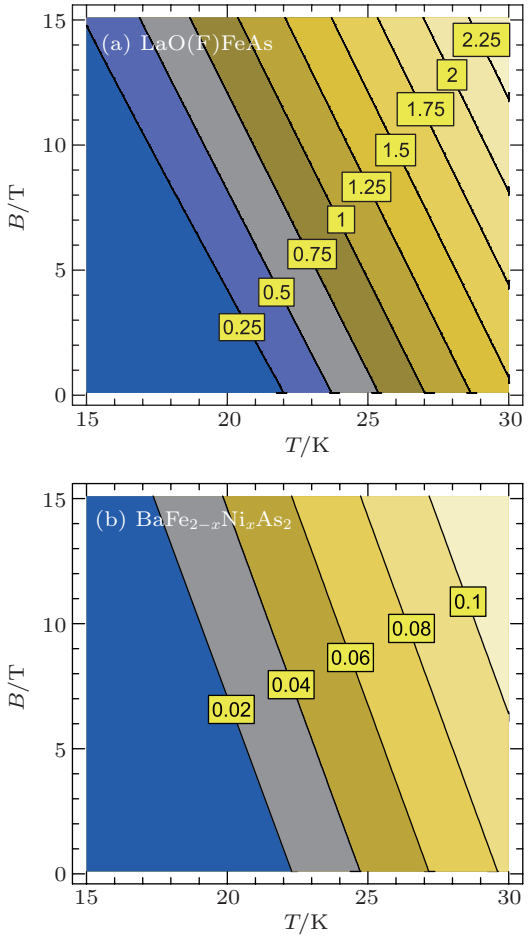


Fig. 3. (color online) The contour lines of εd^2 versus both temperature and magnetic field. (a) For LaOFeAs, $\varepsilon d^2 \sim 1$. (b) For $BaFe_{2-x}Ni_xAs_2$, $\varepsilon d^2 < 1$.

4. Conclusion

We have investigated the superconducting fluctuation electrical conductivity using SCGT of the Lawrence–Doniach Ginzburg–Landau (LDGL) model. The theoretical results can fit very well with the experimental data of iron-based superconductors in a wide region around T_c. Therefore, the cuprates and iron pnictides superconductors with a layered structure can be well described by the LDGL model. Furthermore, other transport effects of these HTSCs, such as Hall conductivity, the Seebeck effect, and Nernst signal, can also be calculated within the LDGL model.

There are three regions in the H–T phase diagram for cuprates and iron pnictides, i.e., 3D, 2D, and their crossover regions. Although different iron-based superconductors share similar layered structures, the dimensionality could be different. LaOFeAs has strong thermal fluctuations near T_c, so in the H–T phase diagram of this family, the 2D region and the crossover region are relatively large, which proves that LaOFeAs has strong layered or 2D characteristics. $BaFe_{2-x}Ni_xAs_2$ has less fluctuation near T_c, so the 2D region and the crossover region are quite small. $BaFe_{2-x}Ni_xAs_2$ is therefore more of a 3D feature. Considering the dimensionality of LiFeAs discussed in the introduction, we can expect it to show a 3D feature near T_c. For a more specific discussion about the dimensionality of LiFeAs above T_c^{mf}, one should use SCGT.

Acknowledgment

We thank Xujiang Jiang and Prof. Zhongshui Ma for discussions.

References

[1] Dai P C 2015 *Rev. Mod. Phys.* **87** 855
[2] Stewart G R 2011 *Rev. Mod. Phys.* **83** 1589
[3] Yang J, Zhou R, Wei L L, Yang H X, Li J Q, Zhao Z X and Zheng G Q 2015 *Chin. Phys. Lett.* **32** 107401
[4] Ye Z R, Zhang Y, Xie B P and Feng D L 2013 *Chin. Phys. B* **22** 087407
[5] Zhu J, Wang Z S, Wang Z Y, Hou X Y, Luo H Q, Lu X Y, Li C H, Shan L, Wen H H and Ren C 2015 *Chin. Phys. Lett.* **32** 077401
[6] Mu G, Zhu X Y, Fang L, Shan L, Ren C and Wen H H 2008 *Chin. Phys. Lett.* **25** 02221
[7] Jiang H, Sun Y L, Xu Z A and Cao G H 2013 *Chin. Phys. B* **22** 87410
[8] Salem-Sugui J S, Alvarenga A D, Rey R I, Mosqueira J, Luo H Q and Lu X Y 2013 *Supercond. Sci. Technol.* **26** 125019
[9] Lebègue S 2007 *Phys. Rev. B* **75** 035110
[10] Pallecchi I, Fanciulli C, Tropeano M, Palenzona A, Ferretti M, Malagoli A, Martinelli A, Sheikin I, Putti M and Ferdeghini C 2009 *Phys. Rev. B* **79** 104515
[11] Rullier-Albenque F, Colson D, Forget A and Alloul H 2012 *Phys. Rev. Lett.* **109** 187005
[12] Fanfarillo L, Benfatto L, Caprara S, Castellani C and Grilli M 2009 *Phys. Rev. B* **79** 172508
[13] Pandya S, Sherif S, Chandra LS S and Ganesan V 2010 *Supercond. Sci. Technol.* **23** 075015
[14] Putti M, Pallecchi I and Bellingeri E, *et al*., 2010 *Supercond. Sci. Technol.* **23** 034003
[15] Liu S L, Gong L Y, Bao G, Wang H Y and Li Y T 2011 *Supercond. Sci. Technol.* **24** 075005
[16] Welp U, Chaparro C, Koshelev A E, Kwok W K, Rydh A, Zhigadlo N D, Karpinski J and Weyeneth S 2011 *Phys. Rev. B* **83** 100513
[17] Ramos-Álvarez A, Mosqueira J and Vidal F 2015 *Phys. Rev. Lett.* **115** 139701
[18] Jiang X J, Li D P and Rosenstein B 2014 *Phys. Rev. B* **89** 064507
[19] Tinh B D, Li D P and Rosenstein B 2010 *Phys. Rev. B* **81** 224521
[20] Wilson B J and Das M P 2014 *J. Phys. Condens. Matter* **26** 325701
[21] Salas P, Fortes M, Solís M A and Sevilla F J 2016 *Physica C* **524** 37
[22] Koshelev A E and Varlamov A A 2014 *Supercond. Sci. Technol.* **27** 124001
[23] Kogan V G and Schmalian J 2011 *Phys. Rev. B* **83** 054515
[24] Larkin A and Varlamov A 2015 *Theory of Fluctuations in Superconductors* (Boston: Oxford University Press) p. 7–75
[25] Rey R I, Ramos-Álvarez, A, Carballeira C, Mosqueira J, Vidal F, Salem-Sugui J S, Alvarenga A D, Zhang R and Luo H 2014 *Supercond. Sci. Technol.* **27** 075001
[26] Troy R J and Dorsey A T 1993 *Phys. Rev. B* **47** 2715
[27] Chen G F, Li Z, Li G, Zhou J, Wu D, Dong J, Hu W Z, Zheng P, Chen Z J, Yuan H Q, Singleton J, Luo J L and Wang N L 2008 *Phys. Rev. Lett.* **101** 057007
[28] Li G, Grissonnanche G, Yan J Q, McCallum R W, Lograsso T A, Zhou H D and Balicas L 2012 *Phys. Rev. B* **86** 054517
[29] Jia Y, Cheng P, Fang L, Luo H Q, Yang H, Ren C, Shan L, Gu C Z and Wen H H 2008 *Appl. Phys. Lett.* **93** 032503
[30] Chen G F, Li Z, Dong J, Li G, Hu W Z, Zhang X D, Song X H, Zheng P, Wang N L and Luo J L 2008 *Phys. Rev. B* **78** 224512
[31] Hu J and MacDonald A H 1997 *Phys. Rev. B* **56** 2788
[32] Aslamazov L G and Larkin A I 1968 *Phys. Lett. A* **26** 238
[33] Ausloos M and Laurent C 1988 *Phys. Rev. B* **37** 611
[34] Freitas P P, Tsuei C C and Plaskett T S 1987 *Phys. Rev. B* **36** 833
[35] Oh B, Char K, Kent A D, Naito M, Beasley M R, Geballe T H, Hammond R H, Kapitulnik A and Graybeal J M 1988 *Phys. Rev. B* **37** 7861